

A High-Gain Polarization Reconfigurable Antenna Using Polarization Conversion Metasurface

Xiang Zhang^{1, *}, Chang Chen¹, Shan Jiang¹, Yangyang Wang², and Weidong Chen¹

Abstract—A novel high-gain polarization reconfigurable antenna composed of a polarization conversion metasurface (PCM) and a linearly polarized source patch antenna is presented in this article. The PCM is placed above the source patch antenna with an air gap. The proposed PCM can convert the linear polarization (LP) wave radiated by the source patch antenna to LP wave, right-hand circular polarization (RHCP) wave, and left-hand circular polarization (LHCP) wave by rotating the PCM around the center of the antenna. Meanwhile, the proposed PCM can serve as the partially reflective surface (PRS) of a Fabry-Perot (FP) resonant cavity which can achieve gain enhancement. In order to validate the performance of the proposed design, a prototype antenna is fabricated and measured. Simulated and measured results agree well. From 10.43 GHz to 11.2 GHz, the polarization reconfiguration can be achieved by rotating the PCM to different angles while maintaining the high gain performance simultaneously.

1. INTRODUCTION

In recent years, polarization reconfigurable antennas have attracted much attention due to their potential of improving the ability of wireless communication systems, such as reducing multipath fading losses and expanding the systems' capability. Various methods have been proposed to achieve polarization reconfigurability. One way for polarization reconfigurability is to utilize RF switches (PIN diodes, MEMS switches, etc.) in antenna radiator. PIN diodes are embedded into the slot of the U-slot patch antenna and the polarization state can be altered by tuning the diodes (on or off) [1]. Two PIN diodes are loaded on two square loop slots in the ground plane to minimize the effect of diodes [2]. Another way to achieve polarization reconfigurability is to generate switchable antenna feeding structures. By applying RF switches to feeding networks, the antenna polarization can be switched between different states [3, 4].

Moreover, polarization reconfigurable antennas based on metasurface (MS) have attracted the attention of researchers. MS is the two-dimensional equivalent of metamaterial which has unique properties not normally found in nature and it can be used to realize polarization reconfigurable antennas. Polarization reconfiguration of MS-based antenna is usually achieved through mechanical approaches (i.e., rotating MS). The polarization of the antennas using MS can be reconfigured to linear polarization (LP), right-hand circular polarization (RHCP) and left-hand circular polarization (LHCP) by rotating the MS [5, 6]. In many application scenarios, polarization reconfigurable antennas with high gain are highly desirable. Fabry-Perot (FP) antenna is often adopted to realize gain enhancement since it has the advantages of compact structure and ease of achieving high gain with simple feeding structure. MS is placed above a source antenna and works as the partially reflective surface (PRS) of FP resonant cavity which can achieve gain enhancement [7–9]. Meanwhile, MS can convert the linearly polarized

Received 20 May 2020, Accepted 9 August 2020, Scheduled 22 August 2020

* Corresponding author: Xiang Zhang (xiangzh@mail.ustc.edu.cn).

¹ Key Laboratory of Electromagnetic Space Information, Chinese Academy of Sciences, University of Science and Technology of China, Hefei, Anhui Province 230027, China. ² National University of Defense Technology, Hefei 230037, China.

wave of a source antenna to a circularly polarized output and the circularly polarized FP antenna can be realized. However, the polarization of the antenna in these designs cannot be reconfigured.

In this article, a novel high-gain polarization reconfigurable FP antenna using PCM is proposed. The polarization of the proposed antenna can be reconfigured among LP, RHCP and LHCP by rotating the PCM around the center of the antenna. Moreover, an FP resonant cavity is formed when the PCM is placed above a linearly polarized source patch antenna and the gain enhancement can be achieved. The proposed PCM has two effects: it can achieve polarization reconfiguration by rotating the PCM and it can always work as the PRS to form the FP resonant cavity during the entire rotation (this has not been investigated in previous PCM designs). Utilizing the proposed PCM, the polarization is reconfigured while high gain performance can be maintained simultaneously. To validate the proposed design concept, the proposed antenna is fabricated and characterized to demonstrate the antenna performance.

2. DESIGN OF THE PROPOSED ANTENNA

The structure of the proposed polarization reconfigurable FP antenna using PCM is shown in Figure 1. It consists of a linearly polarized source patch antenna and a PCM. The PCM, served as the PRS of the FP resonant cavity, is placed above the source patch antenna with a distance of H . The polarization reconfiguration of the proposed antenna can be achieved by rotating the PCM to different angles and gain enhancement of the antenna realized by the FP resonance effect can be maintained during the entire rotation.

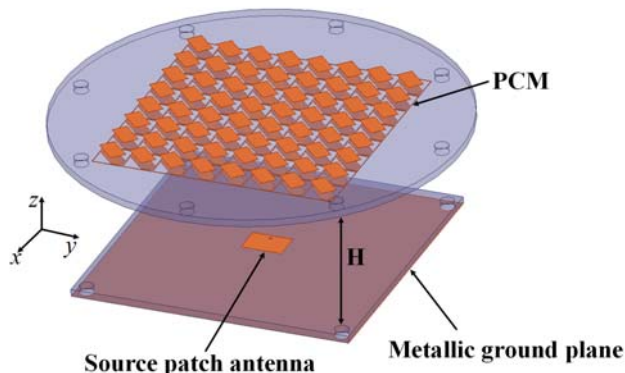


Figure 1. The schematic diagram of the proposed antenna.

2.1. Mechanism of Polarization Reconfiguration

The proposed PCM unit cell is inspired by the PCM in [7]. However, the PCM unit cell in [7] is a multilayer structure which has two substrates and the reflection magnitude is low. Figures 2(a) and (b) depict the geometry of the proposed PCM unit cell. It is composed of one substrate and two metallic layers. The top metallic layer is a rectangular patch while the bottom metallic layer is a square ring with a truncated-corner rectangular patch inside. It can be seen that the geometry of the unit cell is symmetrical with respect to the $+45^\circ$ diagonal direction. When the x -polarized LP wave radiated from the source patch antenna passes through the PCM unit cell (toward the $+z$ -axis direction), the cross-polarization component of the transmitted wave is also quite large since the unit cell is not symmetrical with respect to x -axis. From [10], it is known that when the co-polarization transmission coefficient T_{xx} and the cross-polarization transmission coefficient T_{xy} have the same magnitude but $\pm 90^\circ$ phase difference, the transmitted wave will be circular polarization (CP) wave.

Using the full-wave EM simulation software HFSS, the PCM unit cell is simulated and optimized. As shown in Figure 2(c), a pair of Floquet ports is applied on Port 1 and 2 and the master-slave boundaries are assigned on the sidewalls. The magnitudes of T_{xx} and T_{xy} and their magnitude difference are shown in Figure 3(a). And the phases of T_{xx} and T_{xy} and their phase difference are shown in Figure 3(b).

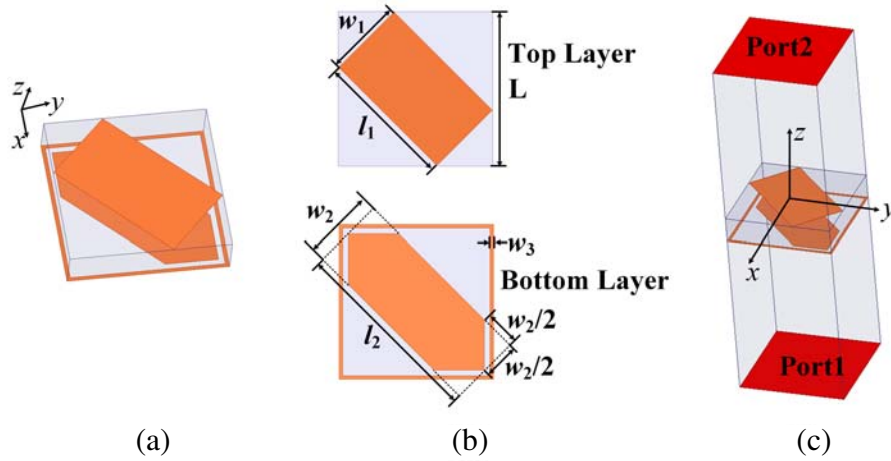


Figure 2. (a) 3-D sketch of the PCM unit cell. (b) Top view of the PCM unit cell. (c) Simulation model of the unit cell. The optimized physical parameters are listed as follows: $L = 6.5$ mm, $l_1 = 5.85$ mm, $w_1 = 3.3$ mm, $l_2 = 8.1$ mm, $w_2 = 3$ mm, $w_3 = 0.15$ mm.

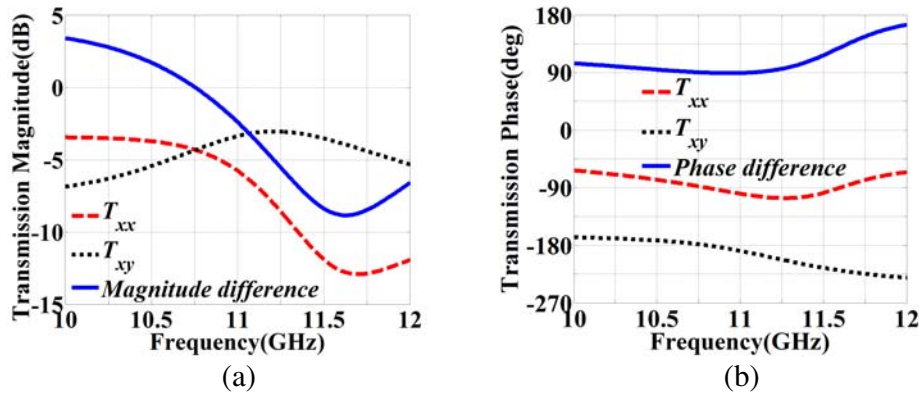


Figure 3. (a) The magnitudes of T_{xx} , T_{xy} and their difference. (b) The phases of T_{xx} , T_{xy} and their difference.

From the simulated results, it can be observed that at 10.75 GHz, the magnitudes of T_{xx} and T_{xy} are the same and the phase of T_{xx} is 90° larger than that of T_{xy} . Thus, the transmitted wave is RHCP wave.

When the unit cell is rotated 45° in the counterclockwise direction, it is symmetrical with respect to x -axis, as shown in Figure 4(a). When the x -polarized LP wave passes through the rotated unit cell, the cross-polarization component of the transmitted wave is quite small and the transmitted wave is still a LP wave. The magnitudes of T_{xx} and T_{xy} are presented in Figure 4(b). The results show that the magnitude of T_{xx} is much larger than that of T_{xy} at 10.75 GHz, and the transmitted wave is x -polarized LP wave.

Similarly, when the unit cell is rotated 90° in the counterclockwise direction, the rotated unit cell is the mirror image of the unit cell since it is symmetrical with respect to the $+45^\circ$ diagonal direction. In this case, the magnitudes of T_{xx} and T_{xy} are the same but the phase of T_{xx} is 90° smaller than that of T_{xy} . The transmitted wave is LHCP wave. When the unit cell is rotated 135° in the counterclockwise direction, the rotated unit cell becomes symmetrical with respect to x -axis again and the transmitted wave is x -polarized LP wave.

In summary, using the proposed PCM (e.g., composed of 8×8 unit cells), the polarization of the antenna can be reconfigurable when the rotation angel θ_R equals 0° , 45° , 90° , and 135° , as shown in Figure 5.

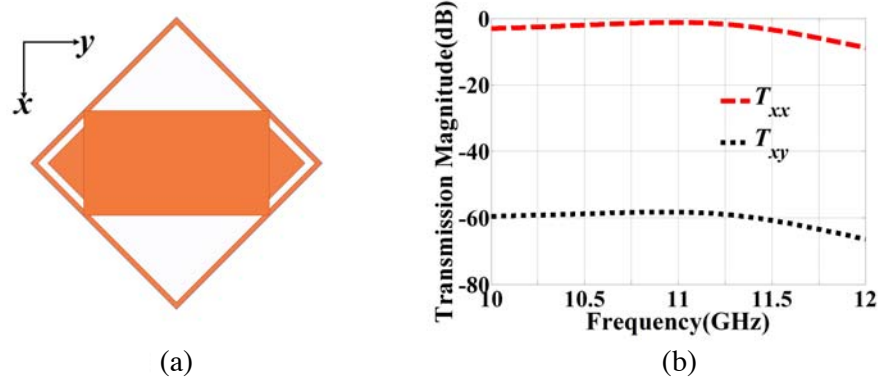


Figure 4. (a) The unit cell which is rotated 45° . (b) The magnitudes of T_{xx} and T_{xy} when the unit cell is rotated 45° .

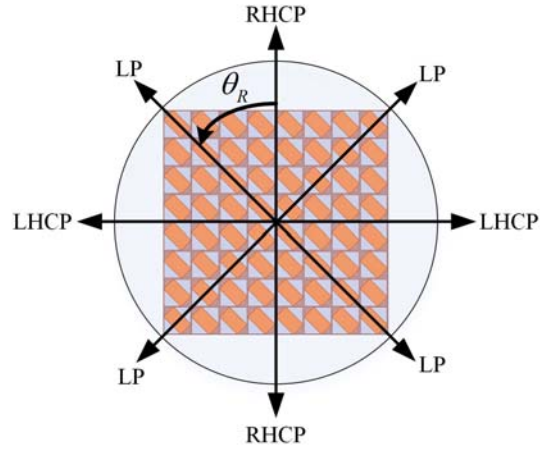


Figure 5. Antenna polarization with different rotation angel θ_R .

2.2. FP Resonance Condition

The PCM which works as PRS can construct an FP resonant cavity with the metallic ground plane of the source patch antenna. The FP resonance effect will contribute to the gain enhancement of the antenna. To realize an FP resonant cavity, the following FP resonance condition must be satisfied:

$$-4\pi H/\lambda + \phi + \varphi = 2N\pi, \quad N = 0, \pm 1, \pm 2 \dots \quad (1)$$

where H is the height of the FP resonant cavity, and λ is the free space wave-length. ϕ and φ are the reflection phases of the PRS and ground plane, respectively.

To keep the high gain performance of the proposed antenna, the FP resonance condition should always be satisfied during the entire rotation. Therefore, the reflection property of the proposed PCM unit cell needs to be investigated. When the rotation angel $\theta_R = 0^\circ$ and 90° , the polarization of the proposed antenna is CP. According to the design method of [11], the FP resonance condition should be satisfied for both the x - and y -polarization components, as given by

$$\begin{cases} -4\pi H/\lambda + \phi_{\theta_R=0^\circ}^x + \varphi_{\text{GND}}^x = 2N\pi \\ -4\pi H/\lambda + \phi_{\theta_R=0^\circ}^y + \varphi_{\text{GND}}^y = 2N\pi \\ -4\pi H/\lambda + \phi_{\theta_R=90^\circ}^x + \varphi_{\text{GND}}^x = 2N\pi \\ -4\pi H/\lambda + \phi_{\theta_R=90^\circ}^y + \varphi_{\text{GND}}^y = 2N\pi \end{cases} \quad (2)$$

where $\phi_{\theta_R=0^\circ}^x$, $\phi_{\theta_R=0^\circ}^y$, $\phi_{\theta_R=90^\circ}^x$ and $\phi_{\theta_R=90^\circ}^y$ are the reflection phases of PCM unit cell for the x - and

y -polarization components when $\theta_R = 0^\circ$ and 90° , respectively. φ_{GND}^x and φ_{GND}^y are the reflection phases of ground plane for the x - and y -polarization components, respectively.

When the rotation angle $\theta_R = 45^\circ$ and 135° , the polarization of the proposed antenna is x -polarized LP, and the FP resonance condition only needs to be satisfied for the x -polarization component

$$\begin{cases} -4\pi H/\lambda + \phi_{\theta_R=45^\circ}^x + \varphi_{\text{GND}}^x = 2N\pi \\ -4\pi H/\lambda + \phi_{\theta_R=135^\circ}^x + \varphi_{\text{GND}}^x = 2N\pi \end{cases} \quad (3)$$

where $\phi_{\theta_R=45^\circ}^x$ and $\phi_{\theta_R=135^\circ}^x$ are the reflection phases of PCM unit cell for the x -polarization components when $\theta_R = 45^\circ$ and 135° , respectively.

Since $\phi_{\theta_R=90^\circ}^x$ and $\phi_{\theta_R=90^\circ}^y$ are the reflection phases of PCM unit cell for the x - and y -polarization components when the unit cell is rotated for 90° , it is known that

$$\begin{cases} \phi_{\theta_R=90^\circ}^x = \phi_{\theta_R=0^\circ}^y \\ \phi_{\theta_R=90^\circ}^y = \phi_{\theta_R=0^\circ}^x \end{cases} \quad (4)$$

The reflection phases of metallic ground plane for the x - and y -polarization components are always equal which means $\varphi_{\text{GND}}^x = \varphi_{\text{GND}}^y$. According to Equations (2)–(4), it leads to

$$\phi_{\theta_R=0^\circ}^x = \phi_{\theta_R=0^\circ}^y = \phi_{\theta_R=45^\circ}^x = \phi_{\theta_R=135^\circ}^x \quad (5)$$

The reflection phase of PCM unit cell should satisfy Equation (5). Figure 6 gives the simulated reflection magnitudes and phases of the proposed PCM unit cell for different polarization components and different rotation angles. From the results, it can be seen that the reflection magnitudes are -5.8 dB at 10.75 GHz for x - and y -polarization components and different θ_R . Meanwhile, the reflection phases $\phi_{\theta_R=0^\circ}^x$, $\phi_{\theta_R=0^\circ}^y$, $\phi_{\theta_R=45^\circ}^x$ and $\phi_{\theta_R=135^\circ}^x$ are the same at 10.75 GHz, equal to -172.2° . Therefore, the FP resonance condition is always satisfied when the PCM is rotated to different angles and the high-gain polarization reconfigurable FP antenna can be designed by using the proposed PCM.

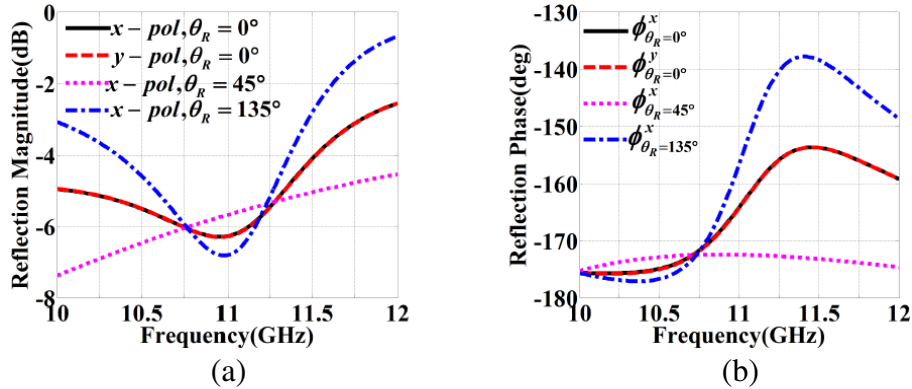


Figure 6. (a) Reflection magnitudes and (b) reflection phases of the proposed PCM unit cell for different polarization components and different rotation angles.

3. RESULTS AND DISCUSSION

A high-gain polarization reconfigurable FP antenna using PCM is fabricated. For ease of rotation, the substrate of PCM is designed as a circle shape (the diameter is 86 mm, the thickness is 1.524 mm). The physical parameters of the proposed PCM unit cell is shown in Figure 2. The source patch antenna is printed on a substrate with the dimensions of 60 mm \times 60 mm \times 1.524 mm. The dimensions of the patch are 6.1 mm \times 8.7 mm. Coaxial probe is used to feed the source patch antenna. The feed point is located 1.05 mm from the edge of the patch (along the center line) and the diameter of the coaxial probe is 0.64 mm. Both substrates use the material of Rogers' RO4350B ($\epsilon_r = 3.66$, $\tan \delta = 0.004$). Four nylon pillars are applied to support the PCM. The height of the FP resonant cavity H is 13.5 mm. The photograph of the fabricated antenna is shown in Figure 7.

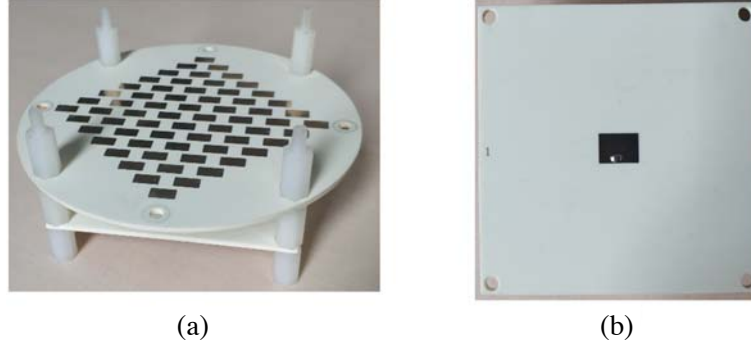


Figure 7. (a) The photograph of the fabricated antenna with PCM. (b) The photograph of the source patch antenna.

3.1. Reflection Coefficient S_{11}

The simulated and measured S_{11} of the proposed antenna with different θ_R are shown in Figure 8. The measured results are consistent with the simulated results. From the measured results, it can be seen that the common frequency band for $S_{11} < -10$ dB is from 10.3 GHz to 11.22 GHz with different rotation angle θ_R .

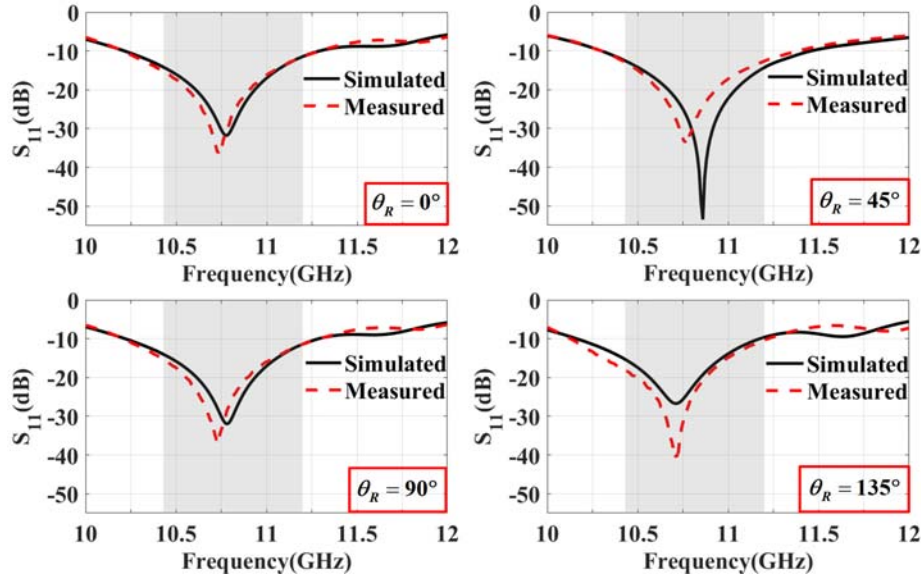


Figure 8. Simulated and measured S_{11} parameters of the proposed antenna with different θ_R .

3.2. Axial Ratio (AR)

Figure 9 presents the simulated and measured ARs with different θ_R . The discrepancies between the measured results and simulated results are mainly caused by the fabrication and measurement tolerance. From the measured results, it can be observed that from 10.43 GHz to 11.2 GHz, the ARs for RHCP and LHCP are lower than 3 dB when $\theta_R = 0^\circ$ and 90° . The ARs are quite large when $\theta_R = 0^\circ$ and 135° and it means that the polarization of the antenna is LP. Therefore, the polarization of the proposed antenna can be reconfigured by rotating the PCM. According to the S_{11} results, the common bandwidth for $S_{11} < -10$ dB and polarization reconfiguration is from 10.43 GHz to 11.2 GHz during the entire rotation.

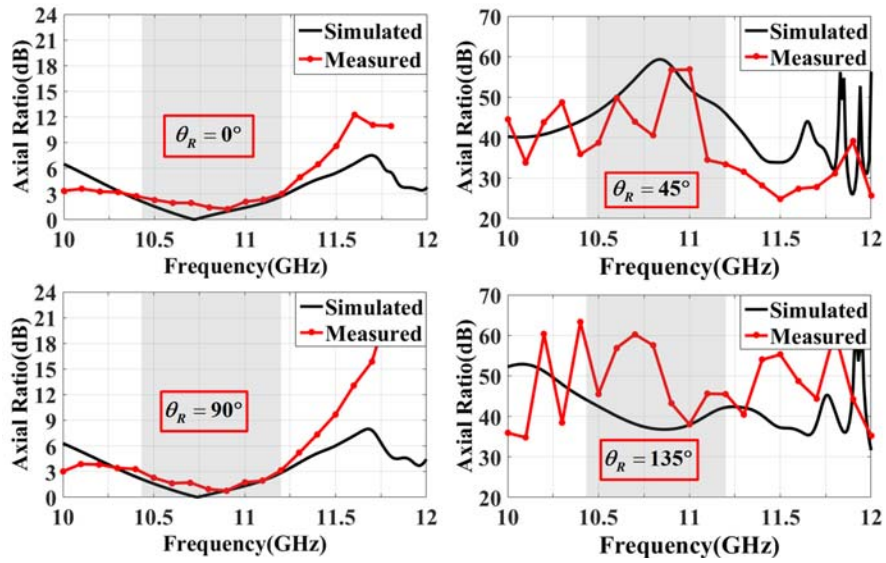


Figure 9. Simulated and measured ARs with different θ_R .

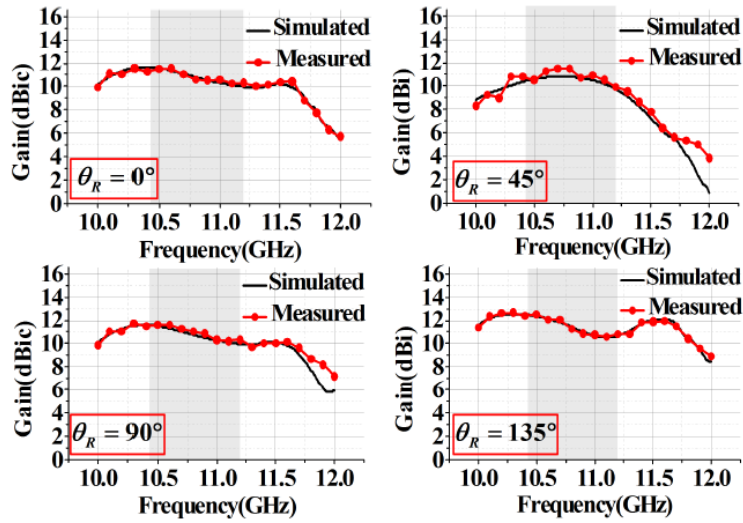


Figure 10. Simulated and measured boresight gains with different θ_R .

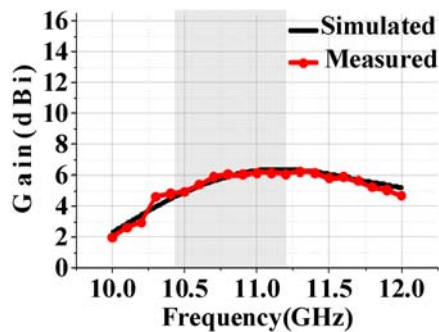


Figure 11. Simulated and measured boresight gain of the source patch antenna.

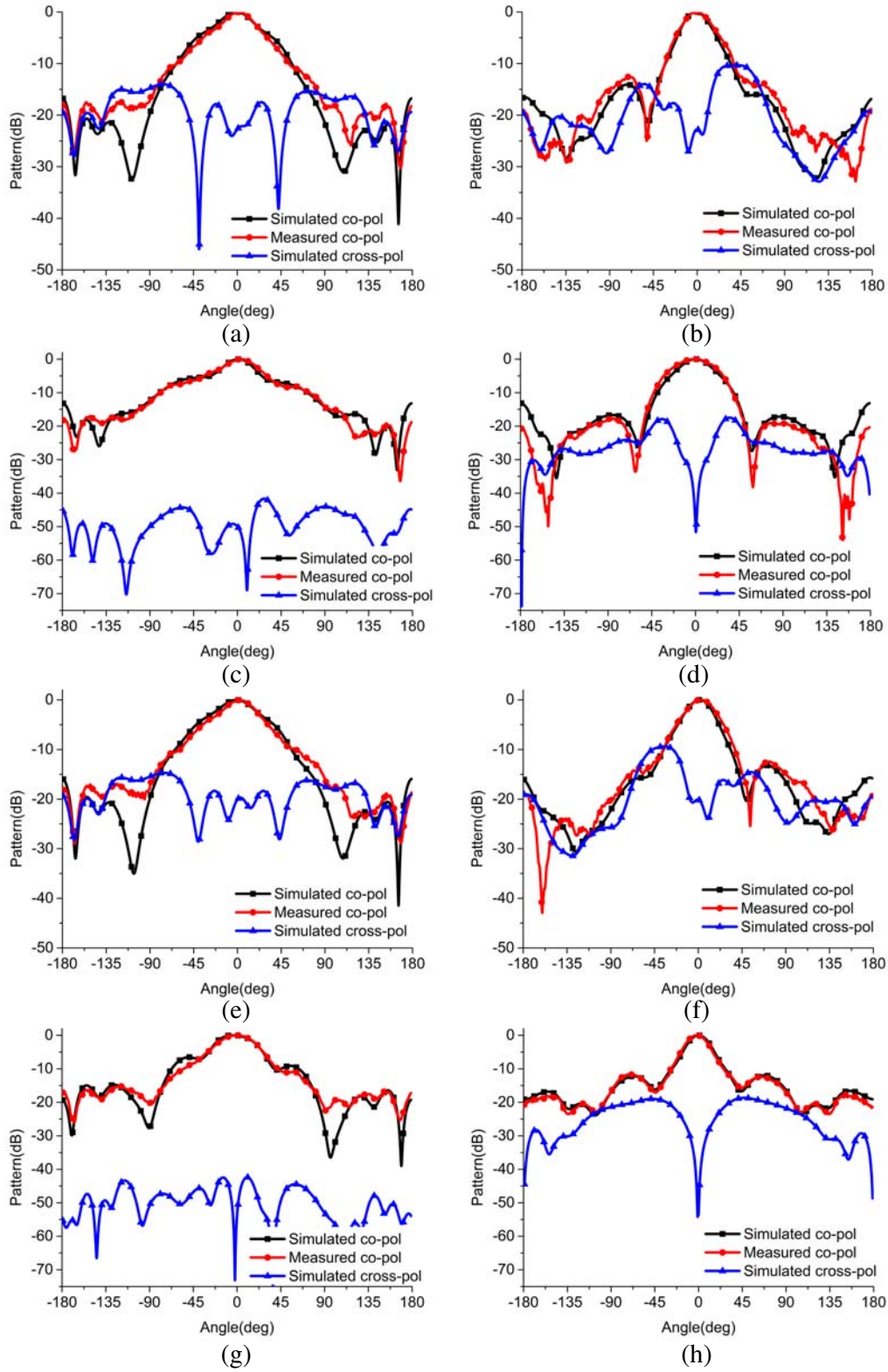


Figure 12. The simulated and measured radiation patterns at 10.9 GHz. (a) $\theta_R = 0^\circ$ xoz -plane, (b) $\theta_R = 0^\circ$ yo z -plane, (c) $\theta_R = 45^\circ$ xoz -plane, (d) $\theta_R = 45^\circ$ yo z -plane, (e) $\theta_R = 90^\circ$ xoz -plane, (f) $\theta_R = 90^\circ$ yo z -plane, (g) $\theta_R = 135^\circ$ xoz -plane, (h) $\theta_R = 135^\circ$ yo z -plane.

3.3. Realized Gain and Radiation Pattern

The simulated and measured realized boresight gains versus frequency with different θ_R are shown in Figure 10. For the purpose of comparison, the gain of the source patch antenna without PCM is presented in Figure 11. It is clear that the antenna gains are enhanced significantly when the PCM is applied. The maximum gain of the proposed antenna is 12.5 dBi during the rotation while the maximum gain of the source patch antenna is 6.2 dBi. During the operating frequency from 10.43 GHz to 11.2 GHz, the gain variation does not exceed 3 dBi or dBic when the PCM is rotated to different angles. The operating frequency range from 10.43 GHz to 11.2 GHz is indicated as dark region, as shown in Figures 8–11. According to the measured gain results, the aperture efficiency of the proposed antenna can be calculated. When rotation angle θ_R is 0° , 45° , 90° , and 135° , the aperture efficiency at 10.75 GHz is 27.87%, 32.37%, 30.14%, and 33.67%, respectively. Figure 12 shows the simulated and measured radiation patterns at 10.9 GHz with different θ_R . The measured co-polarization results agree well with the simulated results. From the simulated cross-polarization results, it can be seen that the cross-polarizations of the proposed antenna with different rotation angle θ_R are less than -20 dB.

4. CONCLUSION

This article presents a high-gain polarization reconfigurable FP antenna using PCM. The antenna is composed of a PCM and a linearly polarized source patch antenna. An FP resonant cavity is formed by the PCM (which serves as PRS) and the ground plane of the source patch antenna. Thus, the gain enhancement can be achieved benefiting from the FP resonance effect. The polarization of the antenna can be configured to LP, RHCP, and LHCP by rotating the PCM to different angles. Meanwhile, the FP resonance condition can always be satisfied utilizing the proposed PCM during the entire rotation. Therefore, polarization reconfiguration and high gain performance can be achieved simultaneously. To validate the design, the proposed antenna is fabricated, and the S_{11} , AR, realized gain, and radiation pattern of the antenna are measured. From the measured results, the polarization of the antenna can be reconfigured from 10.43 GHz to 11.2 GHz, and the gain can be improved significantly over the frequency range.

ACKNOWLEDGMENT

This work was supported by the Fundamental Research Funds for the Central Universities and the Natural Science Foundation of China under Grant 61971392. The authors would like to thank Information Science Laboratory Center of USTC for the measurement services.

REFERENCES

1. Qin, P., A. R. Weily, Y. J. Guo, and C. Liang, "Polarization reconfigurable U-slot patch antenna," *IEEE Transactions on Antennas and Propagation*, Vol. 58, No. 10, 3383–3388, 2010.
2. Yang, X., B. Shao, F. Yang, A. Z. Elsherbeni, and B. Gong, "A polarization reconfigurable patch antenna with loop slots on the ground plane," *IEEE Antennas and Wireless Propagation Letters*, Vol. 11, 69–72, 2012.
3. Wu, Y., C. Wu, D. Lai, and F. Chen, "A reconfigurable quadri-polarization diversity aperture-coupled patch," *IEEE Transactions on Antennas and Propagation*, Vol. 55, No. 3, 1009–1012, 2007.
4. Hu, J., Z. Hao, and W. Hong, "Design of a wideband quad-polarization reconfigurable patch antenna array using a stacked structure," *IEEE Transactions on Antennas and Propagation*, Vol. 65, No. 6, 3014–3023, 2017.
5. Zhu, H. L., S. W. Cheung, X. H. Liu, and T. I. Yuk, "Design of polarization reconfigurable antenna using metasurface," *IEEE Transactions on Antennas and Propagation*, Vol. 62, No. 6, 2891–2898, 2014.

6. Kandasamy, K., B. Majumder, J. Mukherjee, and K. P. Ray, "Low-RCS and polarization-reconfigurable antenna using cross-slot-based metasurface," *IEEE Antennas and Wireless Propagation Letters*, Vol. 14, 1638–1641, 2015.
7. Li, K., Y. Liu, Y. Jia, and Y. J. Guo, "A circularly polarized high-gain antenna with low RCS over a wideband using chessboard polarization conversion metasurfaces," *IEEE Transactions on Antennas and Propagation*, Vol. 65, No. 8, 4288–4292, 2017.
8. Swain, R. and R. K. Mishra, "Metasurface cavity antenna for broadband high-gain circularly polarized radiation," *International Journal of RF and Microwave Computer-Aided Engineering*, Vol. 29, No. 3, e21609, 2019.
9. Xie, P., G. Wang, H. Li, J. Liang, and X. Gao, "Circularly polarized Fabry-Perot antenna employing a receiver-transmitter polarization conversion metasurface," *IEEE Transactions on Antennas and Propagation*, Vol. 68, No. 4, 3213–3218, 2020.
10. Muhammad, S. A., R. Sauleau, L. L. Coq, and H. Legay, "Self-generation of circular polarization using compact Fabry-Perot cavity antennas," *IEEE Antennas and Wireless Propagation Letters*, Vol. 10, 907–910, 2011.
11. Orr, R., G. Goussetis, and V. Fusco, "Design method for circularly polarized Fabry-Perot cavity antennas," *IEEE Transactions on Antennas and Propagation*, Vol. 62, No. 1, 19–26, 2014.